system lymphoma. Arch Ophthalmol 115：1157—1160, 1997.
15) **Akpek EK, Maca SM, Christen WG, Foster S**：Elevated vitreous interleukin-10 level is not diagnostic of intraocular-central nervous system lymphoma. Ophthalmology 106：2291—2295, 1999.
16) **忍足和浩，岡田アナベルあやめ，平形明人**：網膜生検が有用であった眼内悪性リンパ腫の1例. Ophthalmic Surgeons 1：80—81, 2002.
17) **野田航介，鈴木参郎助，安藤靖恭，桂　弘，神園純一，宗司西美，他**：眼と中枢神経系に原発した悪性リンパ腫の9例. 日眼会誌 102：348—354, 1998.
18) **Gass JD, Sever RJ, Grizzard WS, Clarkson JG, Blummenkranz M, Wind CA,** et al：Multifocal pigment epithelial detachments by reticulum cell sarcoma. Retina 4：135—143, 1984
19) **今井和行，吉澤豊久**：中心窩移動術. 田野保雄(編)：眼科診療プラクティス38　黄斑部疾患の外科的治療. 文光堂，東京，72—76, 1998.
20) **田中麻以，後藤　浩，竹内　大，横井秀俊，臼井正彦**：眼内悪性リンパ腫の診断におけるサイトカイン測定の意義. 眼紀 52：392—397, 2001.
21) **政岡則夫，松下久美子，橋田正継，林　暢紹**：眼中枢神経系悪性リンパ腫患者における硝子体中のインターロイキン10とインターロイキン6. 臨眼 54：357—360, 2000.
22) **Hoekzema R, Murray PI, van Haren MA, Helle M, Kijlstra A**：Analysis of interleukin-6 in endotoxin-induced uveitis. Invest Ophthalmol Vis Sci 32：88—95, 1991.
23) **浅尾裕信**：サイトカイン. 宮園浩平，他(編)：サイトカイン・増殖因子実験医学別冊，羊土社，東京，28—39，1995.
24) **Fluckiger AC, Dlurand L, Banchereau J**：Interleukin 10 induces apoptotic cell death of B-chronic lymphocytic leukemia cells. J Exp Medicine 179：91—99, 1994.
25) **Benjamin D, Kuobloch TJ, Dayton MA**：Human B cell interlleukin-10：B cell lines derived from patients with acquired immunodeficiency syndrome and Burkitt's lymphoma constitutively secrete large quantities of interleukin-10. Blood 80：1289—1298, 1992.
26) **Blay JY, Burdin N, Rousset F, Lenoir G, Biron P, Philip T,** et al：Serum interleukin-10 in non-Hodgkin's lymphoma：A prognostic factor. Blood 82：2169—2174, 1993.
27) **Matsuda M, Blankenstein T, Karre K, Kiessling R**：IL-10 converts mouse lymphoma cells to a CTL-resistant, NK-sensitive phenotype with low but peptideinducible MHC class 1 expression. J Immunol 154：6291—6298, 1995.
28) **Bost KL, Bieligk SC, Jaffe BM**：Lymphokine mRNA expression by transplantable murine B lymphocytic malignancies, tumor-derived IL-10 as a possible mechanism for modulating the antitumor response. J Immunol 154：718—729, 1995.
29) **Murray PI, Hoekyma R, van Haren MAC, de Hon FP, Kijlstra A**：Aqueous humor interleukin-6 levels in uveitis. Invest Ophthalmol Vis Sci 31：917—920, 1990.
30) **De Vos AF, Hoekzema R, Kijlstra A**：Cytokines and uveitis, a review. Curr Eye Res. 11：581—597, 1992.
31) **Goldey SH, Stern GA, Oblon DJ, Mendenhall NP, Smith LJ, Duque RE**：Immunophenotypic characterization of an unusual T-cell lymphoma presenting as anterior uveitis. A clinicopathologic case report. Arch Ophthalmol 107：1349—1353, 1989.
32) **el-Shabrawi Y, Livir-Rallatos C, Christen W, Baltatzis S, Foster CS**：High levels of interleukin-12 in the aqueous humor and vitreous of patients with uveitis. Ophthalmology 105：1659—1663, 1998.
33) **Buggage RR, Velez G, Myers-Powell B, Shen DF, Whitcup SM, Chan CC**：Primary intraocular lymphoma with a low interleukin 10 to interleukin 6 ration and heterogeneous IgH gene rearrangement. Arch Ophthalmol 117：1239—1242, 1999.

Graefe's Arch Clin Exp Ophthalmol
(2004) 242:561–565
DOI 10.1007/s00417-004-0878-y

CLINICAL INVESTIGATION

Kei Shinoda
Hisao Ohde
Susumu Ishida
Makoto Inoue
Yoshihisa Oguchi
Yukihiko Mashima

Novel 473-bp deletion in *XLRS1* gene in a Japanese family with X-linked juvenile retinoschisis

Received: 3 November 2003
Revised: 18 December 2003
Accepted: 14 January 2004
Published online: 20 February 2004

K. Shinoda (✉) · H. Ohde · S. Ishida · M. Inoue · Y. Oguchi · Y. Mashima
Department of Ophthalmology,
Keio University School of Medicine,
35 Shinanomachi, Shinjuku-ku,
160-8582 Tokyo, Japan
e-mail: shinodak@uni.de
Tel.: +81-3-33531211 ext. 62402
Fax: +81-3-33598302

Abstract *Purpose:* To present the clinical features of two brothers with molecularly confirmed X-linked juvenile retinoschisis (xlRS) but with non-characteristic electrophysiological findings. *Methods:* Comprehensive ophthalmological examinations were performed. The electroretinograms (ERGs) were recorded under ISCEV standards, and ERGs elicited by long-duration stimuli were also evaluated. Standard genetic analysis of peripheral blood leukocytes was performed. *Results:* Molecular testing revealed a novel 473-bp deletion including exon 4 in the *XLRS1* gene in both siblings. This resulted in a frameshift mutation and a premature termination at codon 78. The scotopic and photopic ERGs were reduced, but the 'negative-type' ERG, characteristic of xlRS, was not observed. Flicker ERGs were also highly reduced. Long-duration stimuli elicited ERGs with a complete loss of the b-wave and a preservation of the off-response, i.e., negative-type ERG. The phenotype/genotype relationship was not determined. *Conclusion:* The consistency of the ERGs elicited by long-duration stimuli in xlRS patients suggests that this type of stimuli provides responses that are a better indicator for the progression or stage of the disease.

Introduction

X-linked juvenile retinoschisis (xlRS, McKusick no. 31270) is one of the more common causes of macular degeneration in young men [6]. Pathognomonic of this disease is a splitting of the nerve fiber layer with vitreal degeneration accompanied by microcystic macular degeneration and the appearance of large holes in the peripheral ablated retinal leaf [8, 31]. Although the exact pathogenesis of the retinal lesions is unknown, the findings of histopathological [5, 14] and electrophysiological studies suggest that the lesions are related to a defect in the retinal Müller cells [17].

The recently identified retinoschisis gene, *XLRS1*, has six exons that encode a 224-amino acid protein, including a 23-residue secretory leader sequence that mediates protein export [20]. The mature protein contains a highly conserved discoidin domain that has been implicated in phospholipid binding and cell–cell interactions on membrane surfaces [20, 27]. The missense mutations found in patients with xlRS are not distributed randomly over the gene but are clustered in the putative discoidin domain, highlighting the biologic importance of this region of the protein [15, 28].

Electrophysiologically, xlRS patients have abnormal electroretinography (ERG) findings, including a characteristic electronegative-type of ERG elicited by a bright flash. Thus, the ERG has been used to make the diagnosis of xlRS [9, 12, 16, 17]. However, the ERG findings can vary in different cases.

Several new findings have been reported in patients with xlRS, e.g., the predominant reduction of the on-response of the photopic long-duration ERG [1], an accompanying impairment in the off-pathway [2, 13, 23], and abnormal photoreceptor function [3, 13]. Because the ERG findings are used almost universally for the diagnosis of xlRS, evaluation on the ERG findings in patients with genetically confirmed xlRS is very important for

determining the mechanism of the disorder and for the phenotype/genotype relationships.

We have reported 11 mutations, including five novel mutations, in the *XLRS1* gene in 12 unrelated Japanese patients with xlRS, and have presented the clinical and electrophysiological findings in these patients [15, 22, 23].

We present the electrophysiological features of two additional Japanese siblings who harbored a novel mutation, a 473 bp deletion in exons 4 and 5 in the *XLRS1* gene. Most interesting was that these two individuals had ERG findings that were not typical of xlRS.

Methods

Amplification with determination of nucleotide sequence

After the two brothers had provided informed consent for participation, genomic DNA was extracted from their peripheral blood leukocytes by standard methods. Individual exons (exons 1–6) of the *XLRS1* gene were amplified by polymerase chain reaction (PCR) using described primers [20].

PCR-amplified products were obtained in all exonal regions except the exon 4 region. Then, a long PCR reaction was performed using sense primer for exon 4 and antisense primer for exon 5. PCR-amplified product was obtained for a shortened length of approximately 400 bp compared with that in a normal subject. We used new intron primers for the sequencing analysis with forward primer in intron 3 (5'-TCCGAAGCGCAAAGCAGATGGG-3') and with reverse primer in intron 4 (5'-CATCTCTCCCCCAGCACTCATA-3').

Direct sequencing of the PCR-amplified products was performed on both strands with an automatic fluorometric 377 DNA sequencer (Applied Biosystems) and a PRISM DyeDeoxy Terminator cycle sequencing kit (Applied Biosystems), following the manufacturer's recommendations.

Electroretinography

Details of the ERG recordings have been presented [24]. Briefly, a bipolar, contact lens electrode carrying light-emitting diodes (LED) was used for the recordings. The ground electrode was attached to the ear. Scotopic, photopic, bright-flash, and 30-Hz-flicker ERGs were recorded in conformity to the ISCEV protocol. On- and off-responses were recorded with the following stimulus parameters; luminance was 300 cd/m^2 on a steady background of 40 cd/m^2, duration was 150 ms, frequency was controlled manually at about 0.3 Hz, and four flashes were averaged. The recording bandpass was 0.5–100 Hz.

Case reports

Case 1

A 4-year-old boy was referred from a local eye clinic to Keio University Hospital in 1984 for a diagnostic evaluation of macular degeneration in both fundi. His corrected visual acuity was 0.15 in the right eye and 0.4 in the left eye. Spectacles were prescribed to correct the hyperopia of +4.5 diopters (D) for the right eye and +2.5 D for the left eye. The anterior segment and the intraocular pressure of each eye were normal. Fundoscopic examination showed typical foveal schisis and peripheral retinoschisis in the temporal regions of each eye. He was diagnosed clinically as having xlRS.

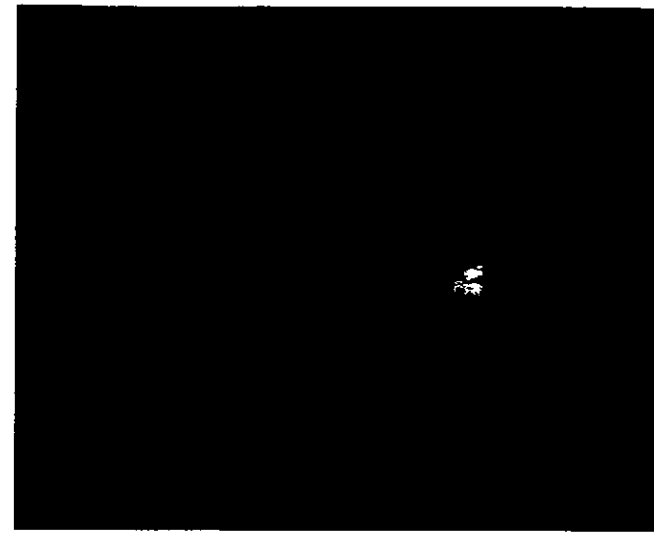

Fig. 1 Photograph of the fundus in case 1 at the age of 23. Blunted foveal reflex is observed in the right eye

At age 11 years in 1991, his corrected visual acuity was 0.4 in the right eye and 0.6 in the left eye. In September 2003, at the age of 23, his corrected visual acuity had decreased to 0.3 in each eye, but the fundoscopic findings remained unchanged during the 19 years of observation at our clinic (Fig. 1).

The scotopic ERGs were reduced (40–60% of controls) but the waveforms were normal. The b/a ratio was 0.95 in the right eye and 1.33 in the left eye for the bright-flash ERGs after 30 min of dark adaptation. The photopic ERGs were abnormal with the b-wave amplitude reduced to approximately 40% of controls. The 30-Hz flicker elicited reduced responses (approximately 30% of controls).

The photopic ERG elicited with long-duration stimuli showed an absent or barely discernible b-wave while the positive d-wave was almost intact at light off, i.e., negative-type ERG.

Direct sequencing analysis of the long PCR-amplified product including exons 4 and 5 revealed a 473-bp deletion in exon 4 and a loss of 34 bp at the end of intron 3, the loss of 142 bp of exon 4, and the loss of 297 bp at the beginning of intron 4 (Fig. 2). A 473-bp deletion including the exon 4 region probably produced a frame-shift mutation at the mRNA level, which resulted in a premature termination at codon 78 and truncation of the protein. Direct sequencing of the PCR-amplified products of the rest of the five exonal regions excluding exon 4 revealed no mutational changes.

Case 2

Case 2 was the younger brother of case 1, and he first visited Keio University Hospital in 1989 when he was 5 years old. He complained of a decrease in vision, which was measured to be 0.7 with +2.5 D in each eye. The anterior segment and the intraocular pressure were normal in both eyes. Ophthalmoscopic examination showed no remarkable findings except for bilateral foveal retinoschisis.

In August 2003, at the age of 19, his corrected visual acuity had decreased to 0.5 in both eyes, whereas the fundoscopic findings had remained unchanged for the 14 years since his first visit.

The scotopic b-wave was reduced to approximately 40% of the control, and the b/a ratio was 1.10 in the right eye and 1.28 in the left eye for the bright-flash ERGs (Fig. 3). The implicit times were

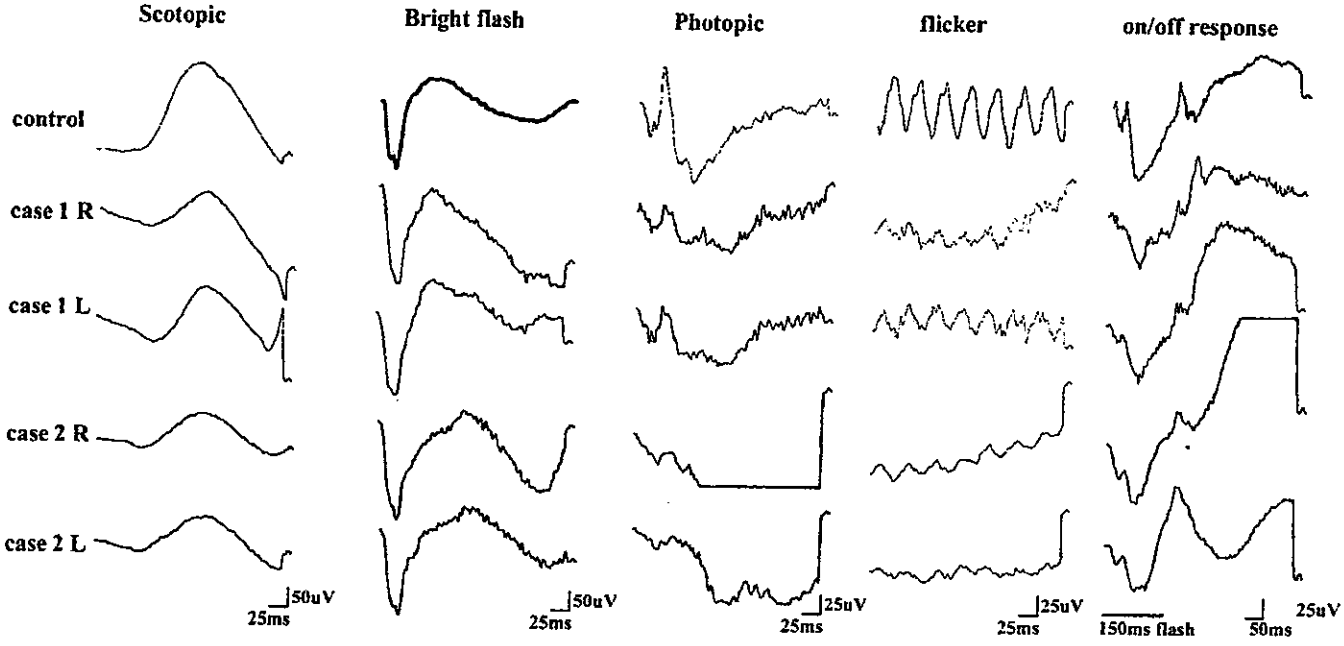

Fig. 3 ERGs recorded according to ISCEV protocol and on- and off-responses in cases 1 and 2. Scotopic ERGs have reduced rod b-waves. Bright-flash ERGs do not show the characteristic "electronegative" appearance, demonstrating a relative preservation of the positive-going b-wave as well as the negative-going a-wave. However, photopic ERGs show a negative-going a-wave but the b-wave is highly depressed. The ERG elicited by 30-Hz flicker stimuli is highly reduced. The photopic ERGs elicited with a long-duration stimulus show negative a-wave and a highly reduced b-wave at light on, while positive d-wave is present at light off

More than 100 mutations of the *XLRS1* gene have been discovered worldwide, and the disease has been reported to have mutational heterogeneity [11, 15, 22, 25, 26, 28]. Although the phenotype/genotype correlation has been studied [11, 22, 26], the relationship remains unclear. Severe cases of xlRS are usually associated with upstream deletions (exons 1–3) in the *XLRS1* gene which prevent the formation of functional mRNA [11, 22]. The mild cases have relatively well preserved visual function and are usually associated with downstream deletions (exon 4). The mutation sites overlap the discoidin-homology domain. However, patients with certain genetic defects can be those who present with severe xlRS [26], as opposed to those with other genetic defects that show a more benign, slowly progressive course. Future studies on larger numbers of patients are necessary to determine the phenotype/genotype correlation in this disease. Investigations on separating the mild and severe cases would probably be helpful.

Electrophysiologically, it is generally accepted that a negative-type ERG is typical in cases of xlRS [9, 12, 16, 17]. Interestingly, in our cases bright-flash ERGs did not show the typical negative-type ERG. Sieving et al. [25] presented an interesting case that was molecularly confirmed as xlRS and showed normal scotopic b-wave to the dim blue light as well as to the bright white flash. The b/a ratio was within the normal range, and the photopic b-wave was also normal. The investigators concluded that ERGs were not an infallible indicator of the disease. Bradshaw et al. [3] analyzed both the rod and cone isolated responses to a wide range of stimulus intensities in patients with xlRS and found an unexpected diversity of amplitudes and waveforms of the dark-adapted ERGs. They also reported that the cone ERGs were abnormal in all patients, and the overall pattern of abnormality suggested a primary inner retinal dysfunction rather than photoreceptor degeneration. Our cases had highly depressed photopic and scotopic ERGs, which agreed with Bradshaw's findings. Additionally, the siblings showed highly depressed flicker ERGs, which is consistent with a previous report [1], supporting the idea of a primary inner retinal dysfunction because the inner retinal contribution to the photopic fast-flicker ERG has been reported [4].

All of these findings indicate that there is wide variability in the electrophysiological and clinical features of xlRS. However, our current patients demonstrated a severe depression of the b-wave with less affected a- and d-waves in ERGs elicited by long-duration stimuli, which is in good agreement with previously reported cases [2, 13, 23]. Given that long-duration stimuli allow evaluations of the on- and off-responses separately, the knowledge that the b-wave reflects mainly the on-pathway was helpful to detect predominantly affected on-pathway function, which would be masked by relatively preserved off-responses when elicited by a short-duration stimulus in the current patients, who showed relatively intact b-

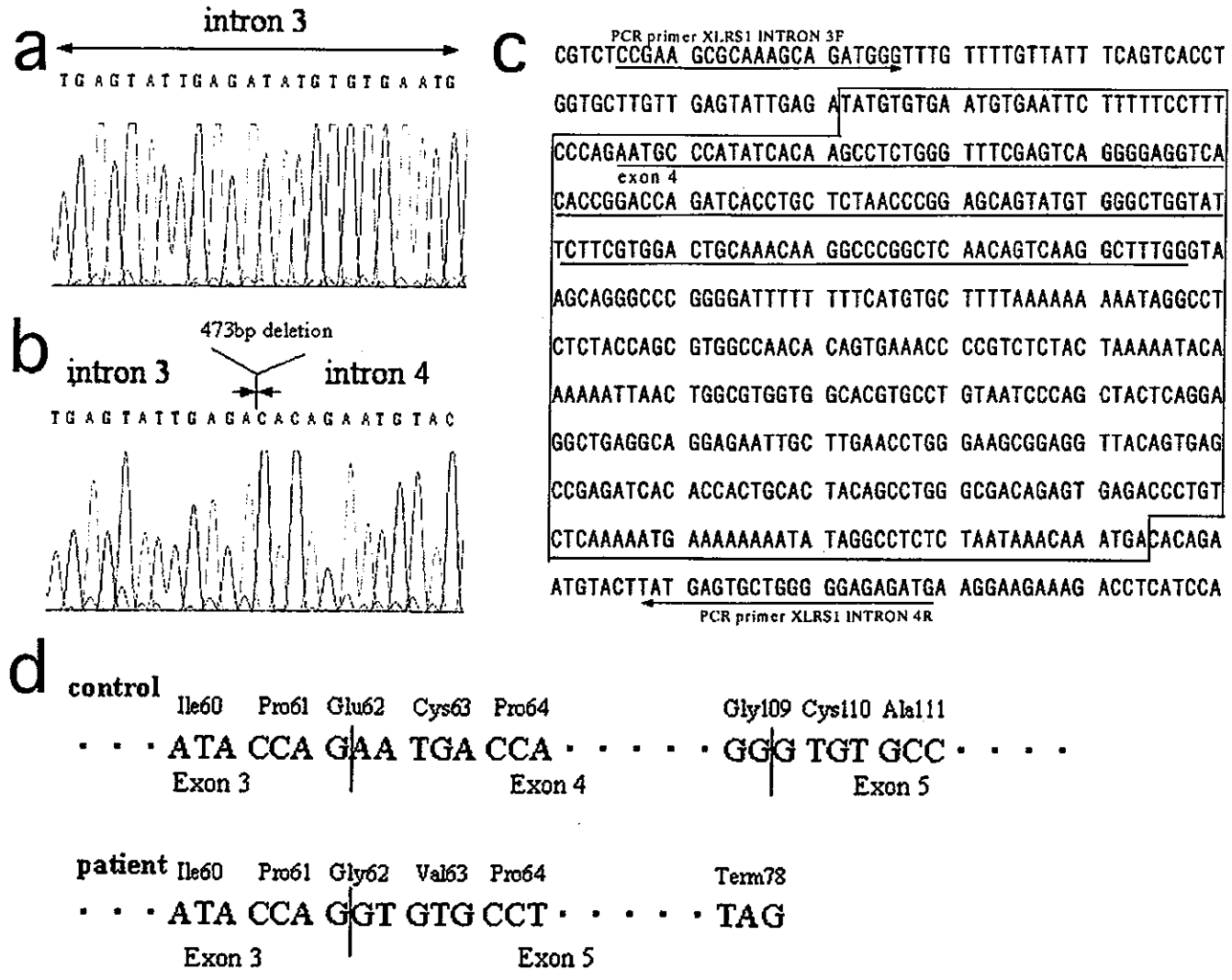

Fig. 2a–d Identification of a deletion in the *XLRS1* gene in case 1. **a** Sequence of intron 3 in wild type. **b** Sequence of intron 3 demonstrating a 473-bp deletion including the region of exon 4 and part of intron 4. **c** *XLRS1* gene sequence showing the deletion area. Exon 4 is *underlined*. The sequences within the *black box* indicate the deletion area (473-bp). **d** Deletion of the exon 4 region produced frameshift mutation at the mRNA level, which resulted in a premature termination at codon 78 and truncation of protein

delayed and the ascending slope of the b-wave was smooth without signs of oscillatory potentials. The photopic ERGs were reduced to less than 20% of the control. The 30-Hz-flicker responses were also markedly reduced so that reasonable measurements of the amplitude could not be made. The ERGs recorded with long-duration stimuli showed a- and d-waves with highly reduced b-waves, i.e., negative-type ERG.

Direct sequencing analysis showed the same mutation as in case 1 (Fig. 2).

Discussion

The clinical features of large series of patients with xlRS from different countries have been reported [6, 10, 12], and the patients have demonstrated a wide range of phenotypes. xlRS was initially thought to be progressive [6], but recent studies have suggested that vision may remain reasonably stable unless severe complications occur [10, 12]. These complications included vitreous hemorrhage, retinal detachment, and neovascular glaucoma, which often require surgical intervention. At present, only limited information is available on the results of surgical treatments [7, 18, 19, 21].

The widely varying phenotypes can be classified into two large groups in terms of treatment: the first group demonstrated the typical course with no surgical indications (mild type) [9, 12], and the second group had severe vision-threatening vitreoretinal pathology requiring surgery (severe type) [7, 18, 19, 21].

wave in the bright-flash ERGs, i.e., no typical negative-type ERG. This is further supported by the selective reduction of the S-cone response [29, 30], because S-cones are found only in the on-pathway. Evaluation of the on-pathway function might provide reliable information for the progression or stage of xlRS.

References

1. Alexander KR, Fishman GA, Grover S (2000) Temporal frequency deficits in the electroretinogram of the cone system in X-linked retinoschisis. Vision Res 40:2861–2868
2. Alexander KR, Fishman GA, Barnes CS, Grover S (2001) On-response deficit in the electroretinogram of the cone system in X-linked retinoschisis. Invest Ophthalmol Vis Sci 42:453–459
3. Bradshaw K, George N, Moore A, Trump D (1999) Mutations of the XLRS1 gene cause abnormalities of photoreceptor as well as inner retinal responses of the ERG. Doc Ophthalmol 98:153–173
4. Bush RA, Sieving PA (1996) Inner retinal contributions to the primate photopic fast flicker electroretinogram. J Opt Soc Am A 13:557–565
5. Condon GP, Brownstein S, Wang NS, Kearns JA, Ewing CC (1986) Congenital hereditary (juvenile X-linked) retinoschisis Histopathologic and ultrastructural findings in three eyes. Arch Ophthalmol 104:576–583
6. Deutman AF. Sex-linked juvenile retinoschisis (1971) In: Deutman AF (ed) The hereditary dystrophies of the posterior pole of the eye. Van Gorcum, Assen, The Netherlands, pp 48–98
7. Ferrone PJ, Trese MT, Lewis H (1997) Vitreoretinal surgery for complications of congenital retinoschisis. Am J Ophthalmol 123:742–747
8. Geiser EP, Falls HF (1961) Hereditary retinoschisis. Am J Ophthalmol 51:1193–1200
9. George ND, Yates JR, Bradshaw K, Moore AT (1995) Infantile presentation of X linked retinoschisis. Br J Ophthalmol 79:653–657
10. George NDL, Yates JRW, Moore AT (1996) Clinical features in affected males with X-linked retinoschisis. Arch Ophthalmol 114:274–280
11. Hiriyanna KT, Bingham EL, Yashar D, Kemp JA, Richards J, Sieving PA (1999) X-linked retinoschisis: XLRS1 gene mutation spectrum and its correlation to clinical phenotypes. Invest Ophthalmol Vis Sci 40 [Suppl]:S471
12. Kellner U, Brummer S, Foerster MH, Wessing A (1990) X-linked congenital retinoschisis. Graefes Arch Clin Exp Ophthalmol 228:432–437
13. Khan NW, Jamison JA, Kemp JA, Sieving PA (2001) Analysis of photoreceptor function and inner retinal activity in juvenile X-linked retinoschisis. Vision Res 41:3931–3942
14. Manschot WA (1972) Pathology of hereditary juvenile retinoschisis. Arch Ophthalmol 88:131–137
15. Mashima Y, Shinoda K, Ishida S, Ozawa Y, Kudoh J, Iwata T, Oguchi Y, Shimizu N (1999) Identification of four novel mutations of the *XLRS1* gene in Japanese patients with X-linked juvenile retinoschisis. Hum Mutat 13:338 (http://journals.wiley.com/1059–7794/pdf/mutation/234.pdf)
16. Murayama K, Kuo CY, Sieving P (1991) Abnormal threshold ERG responses in X-linked juvenile retinoschisis: evidence for a proximal retinal origin of the human STR. Clin Vision Sci 6:317–322
17. Peachey NS, Fishman GA, Derlacki DJ, Brigell MIG (1987) Psychophysical and electroretinographic findings in X-linked juvenile retinoschisis. Arch Ophthalmol 105:513–516
18. Regillo CD, Tasman WS, Brown GC (1993) Surgical management of complications associated with X-linked retinoschisis. Arch Ophthalmol 111:1080–1086
19. Rosenfeld PJ, Flynn HW Jr, McDonald HR, Rubsamen PE, Smiddy WE, Sipperley JO, Boniuk I, Packer AJ (1998) Outcomes of vitreoretinal surgery in patients with X-linked retinoschisis. Ophthalmic Surg Lasers 29:190–197
20. Sauer CG, Gehrig A, Warneke-Wittstock R, Marquardt A, Ewing CC, Gibson A, Lorenz B, Jurklies B, Weber BH (1997) Positional cloning of the gene associated with X-linked juvenile retinoschisis. Nat Genet 17:164–170
21. Schulman J, Peyman GA, Jednock N, Larson B (1985) Indications for vitrectomy in congenital retinoschisis. Br J Ophthalmol 69:482–486
22. Shinoda K, Ishida S, Oguchi Y, Mashima Y (2000) Clinical characteristics of 14 Japanese patients with X-linked juvenile retinoschisis associated with XLRS1 mutation. Ophthalmic Genet 21:171–180
23. Shinoda K, Ohde H, Mashima Y, Inoue R, Ishida S, Inoue M, Kawashima S, Oguchi Y (2001) On- and off-responses of the photopic electroretinograms in X-linked juvenile retinoschisis. Am J Ophthalmol 131:489–494
24. Shinoda K, Ohde H, Inoue R, Ishida S, Mashima Y, Oguchi Y (2002) ON-pathway disturbance in two siblings. Acta Ophthalmol Scand 80:219–223
25. Sieving PA, Bingham EL, Kemp J, Richards J, Hiriyanna K (1999) Juvenile X-linked retinoschisis from XLRS1 Arg213Trp mutation with preservation of the electroretinogram scotopic b-wave. Am J Ophthalmol 128:179–184
26. Simonelli F, Cennamo G, Ziviello C, Testa F, de Crecchio G, Nesti A, Manitto MP, Ciccodicola A, Banfi S, Brancato R, Rinaldi E (2003) Clinical features of X linked juvenile retinoschisis associated with new mutations in the XLRS1 gene in Italian families. Br J Ophthalmol 87:1130–1134
27. Springer WR, Cooper DN, Barondes SH (1984) Discoidin I is implicated in cell-substratum attachment and ordered cell migration of dictyostelium discoideum and resembles fibronectin. Cell 39:557–564
28. The Retinoschisis Consortium (1998) Functional implications of the spectrum of mutations found in 234 cases with X-linked juvenile retinoschisis. Hum Mol Genet 7:1185–1192
29. Yagasaki K, Miyake Y (1983) Blue cone electroretinogram in subjects with X-chromosomal congenital retinoschisis. Folia Ophthalmol Jpn 34:1468–1475
30. Yamamoto S, Hayashi M, Tsuruoka M, Ogata K, Tsukahara I, Yamamoto T, Takeuchi S (2002) Selective reduction of S-cone response and on-response in the cone electroretinograms of patients with X-linked retinoschisis. Graefes Arch Clin Exp Ophthalmol 240:457–460
31. Yanoff M, Rahn EK, Zimmerman LE (1968) Histopathology of juvenile retinoschisis. Arch Ophthalmol 79:49–53

Jpn J Ophthalmol 2004;48:358–363
© Japanese Ophthalmological Society 2004

DOI 10.1007/s10384-004-0096-5

LABORATORY INVESTIGATION

Retinal Blood Flow in the Macular Area Before and After Scleral Buckling Procedures for Rhegmatogenous Retinal Detachment Without Macular Involvement

Tadahiko Eshita[1,2], Kei Shinoda[1], Itaru Kimura[1], Shizuaki Kitamura[1], Susumu Ishida[1], Makoto Inoue[1], Yukihiko Mashima[1], Hiroshi Katsura[3], and Yoshihisa Oguchi[1]

[1]Department of Ophthalmology, Keio University School of Medicine, Tokyo, Japan; [2]Department of Ophthalmology, Tachikawa Hospital KKR, Tokyo, Japan; [3]Katsura Eye Clinic, Tokyo, Japan

Abstract

Purpose: To investigate retinal microcirculation changes in patients with rhegmatogenous retinal detachment (RRD).

Methods: The tissue blood flow in the macular area was measured in 28 patients with RRD without macular involvement by scanning laser Doppler flowmetry before and after scleral buckling procedures. The mean blood flow (MBF) was calculated by the automatic full-field analysis program. The MBF ratios of the affected eye to the fellow eye (a/f ratio) in patients were compared with those of the right eye to the left eye (R/L ratio) in the control subjects.

Results: The mean preoperative a/f ratio in the patients (0.81 ± 0.11) was lower than the mean R/L ratio in the control subjects (1.02 ± 0.11, $P < 0.0001$) and correlated with the extent of RRD ($P < 0.05$). The mean a/f ratio tended to decrease 2 weeks after surgery (0.72 ± 0.09) and recovered to an almost normal level after 1 month (0.96 ± 0.09). The blood-flow change was not influenced by the type of buckling.

Conclusions: The retinal microcirculation in the macular area was disturbed in RRD patients without macular involvement. It correlated with the extent of the RRD, and subsided 1 month after successful scleral buckling procedures. **Jpn J Ophthalmol** 2004;48:358–363 © Japanese Ophthalmological Society 2004

Key Words: macula, microcirculation, retinal blood flow, rhegmatogenous retinal detachment, scleral buckling procedures

Introduction

Rhegmatogenous retinal detachment (RRD) can be treated with scleral buckling, pneumatic retinopexy, or vitrectomy. Scleral buckling is a well-established surgical procedure and the primary method for the majority of uncomplicated RRD cases, showing high anatomic success rates.

Visual acuity should be well maintained, if surgery is successfully performed before the macula is involved. However, deterioration of macular function after scleral buckling procedures for RRD in patients without macular involvement has been demonstrated by focal macular electroretinogram (ERG),[1] multifocal ERG,[2,3] and Humphrey visual field analyzer.[3] One of the causes for these abnor-

Received: December 9, 2003 / Accepted: April 9, 2004
Correspondence and reprint requests to: Tadahiko Eshita, Department of Ophthalmology, Tachikawa Hospital KKR, 4-2-22 Nishikicho, Tachikawa, Tokyo 190-8531, Japan
e-mail: eshita@1994.jukuin.keio.ac.jp

malities has been suggested to be disturbance of circulation in the retina or choroid by scleral buckling.[4–10] The tissue blood flow in the retina or choroid has been noninvasively measured mainly by laser Doppler velocimetry,[4,5] color Doppler ultrasonography,[6–8] the laser speckle method,[9] and the pulsatile ocular blood flow technique.[10] However, the evaluation of the retinal blood flow in the macular area by these techniques has been difficult. The Heidelberg Retina Flowmeter (HRF, Heidelberg Engineering, Heidelberg, Germany), which combines the technique of laser Doppler flowmetry with laser scanning technology, can measure the blood flow of retinal capillaries and is less affected by choroidal circulation.[11] Therefore, it is a suitable technique for measurement of the blood flow in the macular area.

In this study, we measured the tissue blood flow in the macular area in patients with RRD without macular involvement using the HRF to determine whether the microcirculation in the macular area is altered by RRD and scleral buckling procedures.

Materials and Methods

We examined 28 Japanese patients with RRD without macular involvement, who underwent scleral buckling procedures at Keio University Hospital between September 1999 and May 2001. In all patients, RRD was unilateral and did not extend into the vascular arcade. Twenty healthy subjects served as controls.[12] To minimize the intersession variability, the mean blood flow (MBF) measurements both in patients and control subjects were performed in the same period. Informed consent was obtained from each individual who participated in this study after an explanation of the procedures. Patients and control subjects were excluded if they had a cataract that affected visual acuity, a history of intraocular or laser surgery, or if they had taken any medicine other than postoperative antibiotics and antiinflammatory agents in the 2 weeks prior to the examination. Anamnesis revealed mild systemic hypertension in one patient, but it was well controlled without any medication. Preoperative examinations included blood pressure and blood glucose, and no patient showed abnormal values.

The patients consisted of 17 men and 11 women, aged 18 to 68 years with a mean of 42.8 ± 15.0 years (±SD). The control subjects included 5 men and 15 women, aged 18 to 42 years (23.5 ± 5.9 years). The duration of RRD, from the onset of subjective symptoms to the examination, was from 2 to 90 days with a mean of 35.0 ± 32.7 days. Corrected visual acuity was 20/20 or better in both the affected and fellow eyes in each patient at the time of the blood-flow measurement. Refraction of the patients ranged from −8D to +1D with a mean of −3.4 ± 2.9D in the affected eyes and from −8D to +1D with a mean of −3.3 ± 2.8D in the fellow eyes. These showed no significant difference compared with those of the control subjects, which ranged from −8.5D to −2.5D with a mean of −3.7 ± 2.4D in the right eyes and from −8.5D to −2.5D with a mean of −3.6 ± 2.5D in the left eyes ($P > 0.05$, analysis of variance).

The mean intraocular pressure (IOP) of the patients measured before each examination was 12.9 ± 2.1 mmHg in the affected eye and 13.0 ± 2.1 mmHg in the fellow eye. The mean IOP of the control subjects was 12.2 ± 1.7 mmHg in the right eye and 12.4 ± 1.7 mmHg in the left eye. No statistical difference was found between the two groups ($P > 0.05$, paired t test).

The extent of RRD ranged from 1.0 to 2.5 quadrants with a mean of 1.5 ± 0.5 quadrants. Surgery was performed under local anesthesia in all patients. Scleral buckling procedures included transscleral cryotherapy in all patients, drainage of subretinal fluid in 8 patients, and intravitreal gas injection in 4 patients. Local buckling or encircling was performed in 17 and 11 patients, respectively. All of the buckling materials were placed as exoplants. In local buckling, a silicone sponge (#506 or #501, MIRA, Waltham, MA, USA.) was used for the area of 1.0 to 2.5 quadrants. In encircling procedures, a silicone band (#240, MIRA), in combination with a silicone tire (#277 or 276, MIRA) and a silicone sleeve (#270, MIRA), was used in 7 patients, and a silicone sponge (#506 or #501, MIRA) in 4 patients. No intraoperative complication was encountered. Reattachment of the retina was achieved in all patients in the initial surgery. In both pre- and postoperative examinations, no abnormality inside the vascular arcade, including the macula, was detected through indirect ophthalmoscopy and slit-lamp biomicroscopy using a +90 diopter lens.

The tissue blood flow in the macular area was examined before surgery, and 2 weeks, 1, 3, 6, and 12 months after surgery. Four patients who underwent intravitreal gas injection were examined only before surgery. Following measurement of IOP by applanation tonometry, the blood flow was measured in both eyes by scanning laser Doppler flowmetry (SLDF), using the HRF designed to assess the ocular tissue blood flow. The principle, validity, and reliability of SLDF to measure the ocular blood flow have been described and established.[11,13] The measurement area was divided into a superior and an inferior area around the nasal macula, and measurements were performed at least 3 times in both superior and inferior 10° × 2.5° areas (Fig. 1). Each area had a resolution of 256 points × 64 lines, and each line was scanned 128 times. The MBF was calculated as an indicator of tissue microcirculation by the automatic full-field perfusion image analyzer.[14] Retinal vessels with a diameter greater than 30 μm were automatically excluded from measurement. The MBF values obtained from the superior and the inferior area were averaged, and the MBF ratio of the affected eye to the fellow eye (a/f) was calculated, except when the relationship with the location of RRD was analyzed by evaluating the a/f ratios of the superior and the inferior area separately. In the control subjects, the MBF ratio of the right eye to the left eye (R/L) was calculated instead of the a/f ratio. It has been reported that the a/f ratio can be used to determine changes in retinal circulation by the lack of significant difference in the MBF between the two eyes of normal subjects.[12]

All measurements were performed under pupillary dilatation. Subjects were asked to fixate on a distant target

Jpn J Ophthalmol
Vol 48: 358–363, 2004

during the examination. A controllable fixation point for the fellow eye was used to allow desirable positioning of the examined eye. Several mapped images were then acquired in the superior and inferior areas. Great care was taken to detect repeatedly the corresponding retinal area by using visible vessels as landmarks on the video monitor. In each subject, three or more good-quality images, suitable for evaluation of blood flow, were selected and analyzed. Poor-quality images, mainly due to poor fixation, were excluded.

Statistical Methods

The following results are presented as mean values and standard deviation, unless otherwise indicated. For evaluation of the preoperative condition, the preoperative a/f ratio in the patients was compared with the R/L ratio in the control subjects by unpaired t test. Clinical factors associated with preoperative a/f ratios were determined by multiple regression analysis using age, sex, refraction, duration and extent of RRD, break type, and the location of RRD as independent variables with the preoperative a/f ratio as the dependent variable. The correlation of the preoperative a/f ratio with the extent of RRD was analyzed using Spearman's rank correlation. To assess the relationship between the RRD location and the a/f ratio, a paired t test was performed between the superior and inferior a/f ratios both in the patients with superior RRD and in the patients with inferior RRD. For pre- and postoperative a/f ratios, one-factor analysis of variance (ANOVA) followed by Scheffe's F post hoc test was performed to evaluate differences between all comparisons. In order to evaluate the influence of surgical factors, including type of buckling, drainage of subretinal fluid, and the extent of cryotherapy, the change of the preoperative a/f ratio (baseline) in percent was calculated using the following formula: change in % = (a/f ratio after surgery − a/f ratio at baseline) × 100/(a/f ratio at baseline), and the statistical comparison was performed by unpaired t test. Statistical significance was recognized at $P < 0.05$. The coefficient of variation (CV = SD/mean × 100%) was calculated to evaluate the reproducibility of the MBF measurements. In the control subjects, the CV of the mean MBF of the superior and inferior area was 6.07% and 7.74% in the right and left eye, respectively. The CV in the patients was 6.69% in the affected eye and 6.63% in the fellow eye.

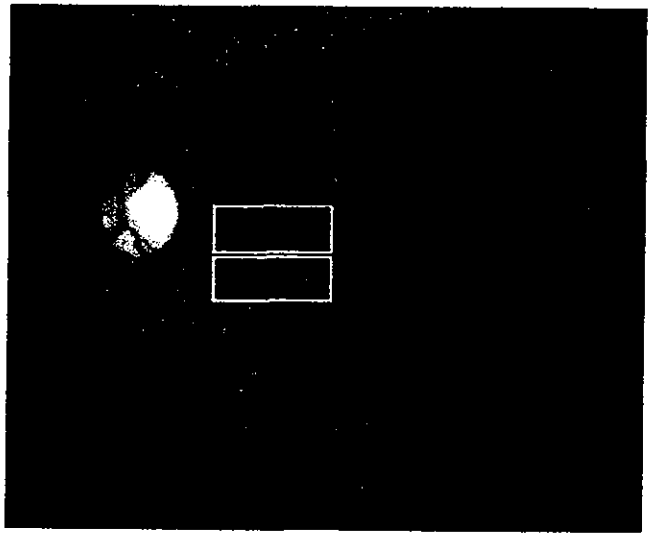

Figure 1. The measurement area was in the macular area was divided into a superior and an inferior section, each 10° × 2.5°. Measurements were performed at least three times for each area. Retinal detachment superior to the vascular arcade is observed.

Results

Blood-flow Changes Before Surgery in Patients with RRD Without Macular Detachment

The mean MBF, a/f ratio in the patients before surgery, and R/L ratio in the control subjects are shown in Table 1. The mean preoperative a/f ratio in the patients was 0.81 ± 0.11, with a range of 0.61–0.98, and was significantly lower than the mean R/L ratio in the control subjects, 1.02 ± 0.11 with a range of 0.76–1.22 ($P < 0.0001$). Multiple regression analysis for several preoperative factors revealed that the preoperative a/f ratio had a significant correlation with the extent of RRD ($P < 0.05$), whereas no correlation was detected with age, sex, refraction, duration or location of RRD, and type of break (Table 2). The a/f ratios in the

Table 1. Mean blood flow in the macular area in patients and control subjects

Patients (n = 28)			Controls (n = 20)		
Affected eye	Fellow eye	a/f ratio	Right eye	Left eye	R/L ratio
226.34 ± 45.29 (134.61–331.72)	283.38 ± 60.07 (178.96–450.19)	0.81 ± 0.11* (0.61–0.98)	282.91 ± 53.50 (209.11–388.63)	278.90 ± 47.68 (208.84–367.57)	1.02 ± 0.11* (0.76–1.22)

Mean blood flow is given in arbitrary units. Data are expressed as mean ± SD (range).
The a/f ratio was defined as the ratio of mean blood flow in an affected eye to that in a fellow eye.
The R/L ratio was defined as the ratio of mean blood flow in the right eye to that in the left eye.
*$P < 0.01$.

Table 2. Multiple regression analysis of factors influencing the preoperative a/f ratio

Variable	Regression coefficient (Significance)
Age	N.S.
Sex	N.S.
Refraction	N.S.
RRD extent	−0.103 (0.021)
RRD location (S or I)	N.S.
RRD location (T or N)	N.S.
Type of break (A or F)	N.S.
RRD duration	N.S.
P value	0.013
Adjusted R^2	0.422

S or I, superior (n = 16) or inferior (n = 12); T or N, temporal (n = 18) or nasal (n = 10); A or F, atrophic hole (n = 13) or flap tear (n = 15); N.S., *not* significant; RRD, rhegmatogenous retinal detachment.

patients with detached retina of 1.0, 1.5, 2.0, and 2.5 quadrants were 0.86 ± 0.16, 0.81 ± 0.07, 0.75 ± 0.08, and 0.70 ± 0.05, respectively. A negative relationship was found between the extent of detached retina and the a/f ratio (Spearman's rank correlation, $\rho = -0.609$, $P = 0.0015$, Fig. 2). In the patients with superior RRD, the superior a/f ratio (0.76 ± 0.11) was lower than the inferior a/f ratio (0.82 ± 0.13). In contrast, in the patients with inferior RRD, the inferior a/f ratio (0.81 ± 0.12) was lower than the superior a/f ratio (0.84 ± 0.12). However, no significant difference was found between the superior and inferior a/f ratios either in the patients with superior RRD or in the patients with inferior RRD.

Blood-flow Changes After Surgery in Patients with RRD Without Macular Detachment

The mean a/f ratios at 2 weeks, 1, 3, 6, and 12 months after surgery were 0.72 ± 0.09, 0.96 ± 0.09, 0.97 ± 0.10, 0.97 ± 0.05, and 0.97 ± 0.02, respectively (Fig. 3). Although the difference did not reach a statistically significant level, the a/f ratio tended to decrease at 2 weeks after surgery. The a/f ratios at 1, 3, 6, and 12 months after surgery were significantly higher than those before surgery, in addition to being higher than the a/f ratio at 2 weeks after surgery (each, $P < 0.05$), suggesting that scleral buckling procedures improved abnormal microcirculation in the macular area in the patients with RRD. In addition, the a/f ratio at 1 month after surgery showed no significant difference when compared with the R/L ratio in the control subjects ($P > 0.05$, unpaired t test). As the MBF recovered to a healthy level after 1 month, we decided to perform further assessments of the effects of several surgical factors on the MBF at both 2 weeks and 1 month postoperatively, using the change in the preoperative a/f ratio (baseline) in percent. There was no significant difference between the two groups classified according to type of buckling, drainage of subretinal fluid, and the extent of cryotherapy at either 2 weeks or 1 month after surgery.

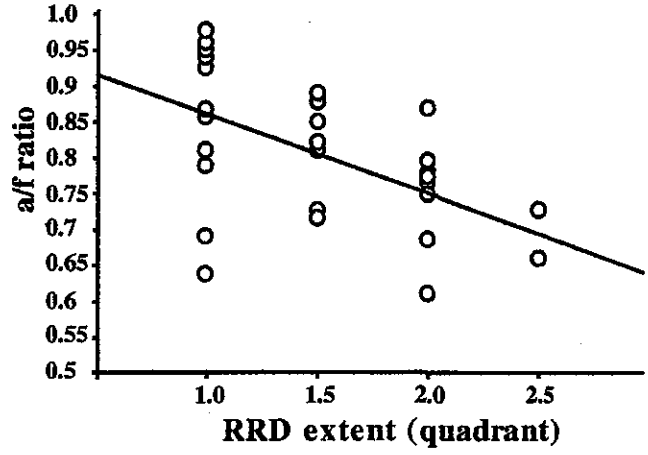

Figure 2. Correlation of the preoperative ratio of the mean blood flow (MBF) of the affected eye to that of the fellow eye (a/f ratio) and the extent of rhegmatogenous retinal detachment (RRD). A negative relationship was demonstrated ($\rho = -0.609$, $P = 0.0015$).

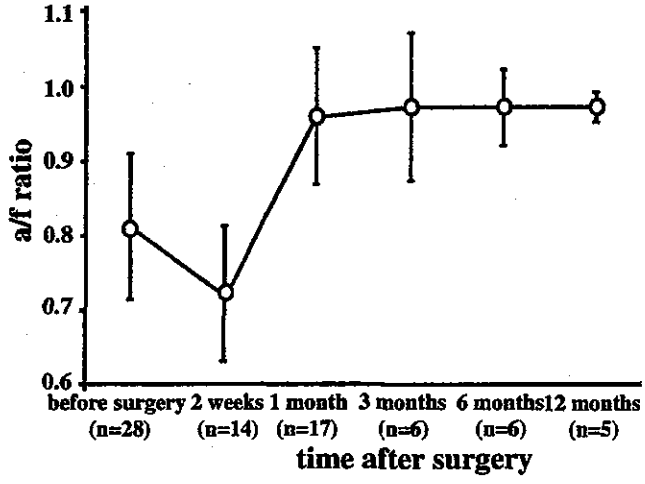

Figure 3. The mean a/f ratios before and at 2 weeks, 1, 3, 6, and 12 months after surgery. The mean a/f ratios at 1, 3, 6, and 12 months after surgery were significantly higher than those before surgery in addition to being higher than the a/f ratio at 2 weeks after surgery (each, $P < 0.05$). Each bar indicates the standard deviation. n, number of samples.

Discussion

The current study is the first to evaluate the retinal blood flow in the macular area by the HRF before and after scleral buckling procedures in the patients with RRD without macular involvement. Interestingly, a reduction in the blood flow was noticed before surgery in the affected eyes, and had a significant correlation with the extent of RRD. Although the control subjects were younger than the patients, association of age with the blood flow was neglected by using a/f and R/L ratios in which the normal

value is 1.0.[12] Normal ocular blood flow in RRD has been reported in several studies,[6,7,9] but the main targets for evaluation were the central retinal artery and the ophthalmic artery[6,7] or choroidal vessels.[9] The blood-flow rate in the major superior and inferior temporal retinal arteries, which were in the attached retinas of the patients with RRD, was measured by the laser Doppler technique.[4,15] It was found to be lower than in the fellow eyes[4] or in the normal controls.[15] In addition, the blood-flow rate in arteries supplying the detached portion of the retina was approximately 30% lower than in arteries supplying the attached portion.[4] In a previous study by Satoh,[16] by a system using videofluorescence angiography and image analysis with the dye dilution technique, retinal mean circulation times of the detached areas were longer than those of the nondetached areas in the patients with RRD, and both were longer than those of normal subjects. These findings suggest that circulatory disturbance in patients with RRD can occur in the entire retina.

Despite falling short of statistical significance compared with that before surgery, the blood flow in the macular area tended to decline at 2 weeks after successful surgery by scleral buckling procedures, and the reduction was not influenced by surgical factors such as type of buckling, drainage of subretinal fluid, or the extent of cryotherapy. At 1 month after surgery, the blood flow recovered to almost normal level, which was maintained throughout the 12-month postoperative study period. Reduction of the blood flow in major retinal arteries,[5] the central retinal artery,[6,7] the ophthalmic artery,[6–8] and the choroid[9,10] after scleral buckling procedures that continued more than several months has been previously demonstrated in numerous investigations, but there has been no report in which the retinal blood flow in the macula was evaluated. Nagahara et al.[9] measured the foveal blood flow in the patients without macular involvement using the laser speckle method and reported that it was normal both before and after surgery. However, the data obtained from the foveal area was assumed to be affected only by choroidal circulation because the area was free from retinal capillaries and the measuring depth was at least 1 mm in the laser speckle technique. In all the above reports, it was suggested that compression on the peripheral vasculature by indentation caused by the scleral buckle, especially the encircling buckle, might be responsible for the reduction of the ocular blood flow. Results from this study, however, indicate that scleral buckling procedures might have only a slight influence on the microcirculation of the nondetached retina in the macular area. Although these results should be carefully interpreted since previous investigations showed different parameters on the different vessels from those in this study, the macular microcirculation might be less susceptible to the compression force, which could persistently affect the blood flow in the main ocular vessels. Abnormal macular function after surgery in cases of RRD without macular involvement detected by multifocal ERG tended to continue for at least 2 months after surgery using the encircling procedure.[2] Regarding the cases in the present study, retinal reattachment surgery normalized the preoperative reduction of the blood flow in 1 month irrespective of the buckle type. This suggests that postoperative circulatory improvement might precede functional recovery.

The ocular blood flow has been measured noninvasively by several techniques. Those include the laser Doppler technique[4,5] applied for major retinal arteries, color Doppler ultrasonography[6–8] for the central retinal artery and the ophthalmic artery, and the laser speckle method[9] and the pulsatile technique,[10] mainly for choroidal vessels. SLDF using the HRF made it possible to measure the capillary blood flow in distinct areas of the retina[11] and therefore was useful for evaluation of microcirculation in the macula. The measuring depth by the HRF is 300 μm, so measurements may have included the choroidal blood flow in the foveola, where the retina is very thin, approximately 135 μm. Comparing the diameter of the foveola, 350 μm, with the measurement area of 10° × 2.5°, which is almost equal to 2.7 × 0.7 mm, however, the contribution of the foveola in the present study would be extremely small.

In ERG studies,[1–3] the b-wave component and oscillatory potential, both of which reflect inner retinal layer function, seemed to be susceptible to scleral buckling procedures. These results support the reduction of the retinal blood flow in the macular area shown in the present study, together with the previous finding by Nagahara et al.[9] in which the foveal choroidal blood flow was normal before and after surgery.

In conclusion, we demonstrated for the first time that the retinal blood flow in the macular area was reduced in RRD even if the macula was not involved and the reduction was recovered after 1 month by scleral buckling procedures. Although corrected visual acuity was maintained at normal levels before and after surgery in our patients, early surgery should be recommended even in cases of peripheral retinal detachment. Recently, vitreous surgery has been primarily indicated for selected cases of RRD,[17] and postoperative reduction of the choroidal blood flow has been reported in vitrectomy cases but less than in scleral buckling cases.[18] The influence of vitreous surgery on microcirculation in the macula and its recovery should also be investigated in the future.

References

1. Horiguchi M, Horiguchi M, Kondo M, Miyake Y, Tomita N. Alteration of macular ERG after scleral buckling in patients with peripheral retinal detachment. Nihon Ganka Kiyo (Folia Ophthalmol Jpn) 1995;46:587–591.
2. Matsuzaki T, Shinoda K, Inoue M, et al. Multifocal electroretinography after scleral buckling for rhegmatogenous retinal detachment. Ganka Shujutu (Jpn J Ophthalmic Surg) 2001;14:391–394.
3. Mori T, Nakajima S, Kato C. The macular function following retinal detachment surgery. Rinsho Ganka (Jpn J Clin Ophthalmol) 1998;52:741–744.
4. Yoshida A, Feke GT, Ogasawara H, et al. Symposium on physiological aspects of retinal detachment. Intraocular circulation following detachment surgery. Ganka Rinsho Iho (Jpn Rev Clin Ophthalmol) 1991;85:2370–2379.

5. Ogasawara H, Feke GT, Yoshida A, Milbocker MT, Weiter JJ, McMeel JW. Retinal blood flow alterations associated with scleral buckling and encircling procedures. Br J Ophthalmol 1992;76: 275–279.
6. Hanioglu-Kargi S, Yazar Z, Ziraman I, Gursel E. Effects of scleral buckling on the retrobulbar haemodynamic changes. Eye 1999;14:165–171.
7. Regillo CD, Sergott RC, Brown GC. Successful scleral buckling procedures decrease central retinal artery blood flow velocity. Ophthalmology 1993;100:1044–1049.
8. Santos L, Capeans C, Gonzalez F, Lorenzo J, Codesido J, Salorio MS. Ocular blood flow velocity reduction after buckling surgery. Graefes Arch Clin Exp Ophthalmol 1994;232:666–669.
9. Nagahara M, Tamaki Y, Araie M, Eguchi S. Effects of scleral buckling and encircling procedures on human optic nerve head and retinochoroidal circulation. Br J Ophthalmol 2000;84:31–36.
10. Yoshida A, Hirokawa H, Ishiko S, Ogasawara H. Ocular circulatory changes following scleral buckling procedures. Br J Ophthalmol 1992;76:529–531.
11. Michelson G, Schmauss B, Langhans MJ, Harazney J, Groh MJM. Principle, validity, and reliability of scanning laser Doppler flowmetry. J Glaucoma 1996;5:99–105.
12. Kimura I, Shinoda K, Tanino T, Ohtake Y, Mashima Y, Oguchi Y. Scanning laser Doppler flowmeter study of retinal blood flow in macular area of healthy volunteers. Br J Ophthalmol 2003; 87:1469–1473.
13. Michelson G, Schmauss B. Two-dimensional mapping of the perfusion of the retina and optic nerve head. Br J Ophthalmol 1995;79:1126–1132.
14. Michelson G, Welzenbach J, Pal I, Harazny J. Automatic full field analysis of perfusion images gained by scanning laser Doppler flowmetry. Br J Ophthalmol 1998;82:1294–1300.
15. Tagawa H, Feke GT, Goger DG, McMeel JW, Furukawa H. Retinal blood flow changes in eyes with rhegmatogenous retinal detachment and scleral buckling procedures. Nippon Ganka Gakkai Zasshi (Acta Soc Ophthalmol Jpn) 1992;96:259–264.
16. Satoh Y. Retinal circulation in rhegmatogenous retinal detachment demonstrated by videofluorescence angiography and image analysis. I. The condition of retinal circulation before retinal detachment surgery. Nippon Ganka Gakkai Zasshi (Acta Soc Ophthalmol Jpn) 1989;93:1002–1008.
17. Heimann H, Bornfeld N, Friedrichs S, Helbig H, Korra A, Foerster MH. Primary vitrectomy without scleral buckling for rhegmatogenous retinal detachment. Graefes Arch Clin Exp Ophthalmol 1996;234:561–568.
18. Vetrugno M, Gigante G, Cardia L. The choroidal circulation after retinal detachment surgery. Clin Hemorheol Microcirc 1999;21: 349–352.

Graefe's Arch Clin Exp Ophthalmol
(2004) 242:587–596

LABORATORY INVESTIGATION

DOI 10.1007/s00417-004-0862-6

Florian Gekeler
Karin Kobuch
Hartmut Normann Schwahn
Alfred Stett
Kei Shinoda
Eberhart Zrenner

Subretinal electrical stimulation of the rabbit retina with acutely implanted electrode arrays

Received: 8 September 2003
Revised: 17 December 2003
Accepted: 29 December 2003
Published online: 5 June 2004

F. Gekeler (✉) · H. N. Schwahn · K. Shinoda · E. Zrenner
University Eye Hospital,
Schleichstrasse 12–16, 72076 Tübingen, Germany
e-mail: gekeler@uni-tuebingen.de
Tel.: +49-7071-2984786
Fax: +49-7071-295038

K. Kobuch
University Eye Hospital,
Regensburg, Germany

A. Stett
Natural and Medical Science Institute,
Reutlingen, Germany

Abstract *Background:* Subretinal implants intend to replace photoreceptor function in patients suffering from degenerative retinal disease by topically applying electrical stimuli from the subretinal space. This study intended to prove the feasibility of a newly developed transchoroidal surgery and, furthermore, of a subretinal electrode array, which closely resembles envisioned human implants to electrically stimulate the visual system in rabbits. *Methods:* Five rabbits (ten eyes) were implanted with a 4×2-electrode array via a transchoroidal access to the subretinal space. The electrodes were connected to an arbitrary stimulus generator to apply voltage pulses. Retinae were accessed by light microscopy after stimulation with various intensities. *Results:* The stimulating foil could be introduced into the subretinal space in all eyes. In seven of ten eyes electrically evoked cortical potentials following subretinal electrical stimulation could be elicited. Threshold voltages ranged from less than 0.1 to 2.38 V with a corresponding threshold charge of approximately 1.0 nC per electrode or 10 $\mu C/cm^2$. Histology revealed localized retinal damage over some of the electrodes succeeding stimulation strengths of 2 V and consistent damage over all electrodes succeeding voltages of 3 V. *Conclusions:* The study demonstrates the feasibility of the transchoroidal surgical access to place subretinal implants in rabbit eyes and provides proof of successful cortical activation following subretinal electrical stimulation by an electrode array envisioned for human implantations.

Introduction

In many degenerative retinal diseases, such as retinitis pigmentosa (RP) and age-related macular degeneration (ARMD), retinal cell death and re-organization ultimately lead to irreversible blindness. There is little debate that the majority of cell loss occurs in the outer nuclear layer (ONL) containing the photoreceptors (PRs) [19, 23, 30]. The inner nuclear layer (INL) and the ganglion cell layer (GCL) in comparison stay relatively intact preserving 20–40% of their neurons depending on the type and stage of the disease and on the eccentricity on the retina. From these results it seems reasonable to expect surviving cell populations in the inner retinal layers which could receive, transform, and transmit electrical signals from the prosthesis via the optic nerve to the brain.

Consistently many studies [2, 3, 4, 6, 7] have demonstrated the possibility to elicit phosphenes by electrical stimulation in healthy persons and in patients blinded by degenerative retinal disease. These studies ultimately raised the concept of a visual prosthesis designed to electrically stimulate the visual system with multi-electrode arrays thereby restoring pattern vision by topically correct excitation at various locations along the visual pathway.

Four main locations for electrical stimulation of the visual system have been proposed: (a) the visual cortex; (b) the optic nerve and the lateral geniculate nucleus

(LGN); (c) the ganglion cell layer (GCL) via an epiretinal prosthesis; and (d) the retinal network via a subretinal prosthesis.

The visual cortex has been activated by variable numbers of electrodes in animals and also humans [3, 4, 8, 9, 10, 11, 24, 25, 29, 31]. The LGN has been accessed [40] as well as the optic nerve [36]. Most experiments with successful electrical stimulation of the visual system have been performed with epiretinal prostheses in animals and humans in acute and chronic experiments [13, 15, 16, 17, 18, 20, 21, 28, 38, 39]. Furthermore, studies have clearly demonstrated the principal feasibility of a subretinal prosthesis [5, 13, 14, 27, 32, 34, 43, 44, 45, 46].

One of the advantages of a subretinal prosthesis is the possibility to utilize the remaining retinal network to process the information initiated by the prosthesis. Furthermore, electrical multisite stimulation from the subretinal space (SRS) comes closest to physiological conditions in terms of stimulation site and would, in the ideal case, not require external cameras and image processing devices to compensate for off-site stimulation, as may be the case in epiretinal prosthesis where GC-fibers from far away in the visual field might be stimulated.

Chow et al. [5] have been able to evoke cortical responses following subretinal electrical stimulation in rabbits by placing a single large electrode under the retina which was connected to a photocell outside of the eye that was illuminated by a bright light flash; however, no studies have thus far examined the exact conditions which are necessary to successfully evoke visual perceptions from the SRS in vivo. To make use of the possible advantages of subretinal prostheses the stimulus characteristics have to be defined more clearly. This prompted us to determine voltage and charge, respectively, by using electrical stimulation with regularly arranged electrodes which more closely resemble future implants. The electrodes were stimulated in a controlled manner by an external stimulus generator to find thresholds of voltage and charge for successful cortical activation as proven by electrically evoked cortical potentials (EECPs) within a range that does not harm the cells stimulated.

Materials and methods

Animals

Five adult Chinchilla Bastard rabbits were included in the study (Charles River GmbH, Germany) with experiments performed on ten eyes. All animal experiments adhered to the "Principles of laboratory animal care" (NIH publication no. 85–23, revised 1985), the OPRR Public Health Service Policy on the Humane Care and Use of Laboratory Animals (revised 1986), and the U.S. Animal Welfare Act, as amended, as well as the local commission for animal welfare.

Anesthesia

Anesthesia was achieved by intramuscular injection of ketamine hydrochloride 10% (Ketavet 10%) and Xylazine 2% (Rompun 2%) in a mixing ratio of 2:1. Initial dose was 50 mg ketamine hydrochloride per kilogram body weight.

Electrophysiological recording electrodes

One epidural stainless steel screw was placed as active electrode epidurally 4 mm anterior and 5 mm lateral on each side of lambda, and the reference electrode was placed epidurally on the midline 25 mm anterior to lambda. A subcutaneous needle electrode at the tip of the nose served as ground electrode.

Surgical technique: transchoroidal implantation of the subretinal foil strip

For implantation, a scleral flap (3×3 mm) was prepared about 6 mm away from the limbus in the upper lateral quadrant of the eye. After local drug-induced vasoconstriction with Suprarenin 1:1000 (Aventis Pharma, Bad Soden, Germany) the choroid was incised along the great vessels with a 27-G needle taking great care not to injure the underlying retina.

The stimulating foil strip was introduced along a previously introduced, custom-made slide rail to the desired position. Time for a single operation was approximately 1 h. After the surgery, the eye was immediately stimulated electrically followed by the same procedure in the other eye within one session before killing and enucleation for histology.

Electrophysiological recordings

For all recordings an Espion Console was used (Diagnosys LLC, Littleton, Mass.). The Pentium-based system provides five 28-bit DC coupled opto-isolated differential input channels. All data were stored on the hard disk for offline analysis. Bandpass filter settings were 0.03 Hz as low and 300 Hz as high cut-off frequency (except for rabbits I and II: 0–1000 Hz). Cortical activity was recorded in response to stimulation of the contralateral retina. For objective assessment of the response to subretinal electrical stimulation the area under the curve (AUC) was calculated for the time period in which a physiological response from the visual cortex was expected (25–200 ms after onset of stimulation). To adjust for the noise level the AUC of the response (25–200 ms) was divided by the AUC of periods without stimulation which yielded an AUC ratio for each stimulus condition. The AUC ratio provides an objective and quantifiable measure of response strength and is independent of the waveform. It is also an objective parameter in all recordings without any discernible waveform (i.e., sub-threshold stimulation). Similar techniques have extensively been used to evaluate ERG and cortical responses (e.g., [12, 13]).

For assessment of the retina and the visual pathway to control effects of surgery or electrical stimulation ganzfeld visual evoked potentials (VEPs) were recorded before surgery and after electrical stimulation of the retina.

Electrostimulation of the retina

For subretinal stimulation an array of thin-film platinum electrodes on a flexible polyimide foil (manufacturer: Fraunhofer Institute for Biomedical Engineering, St. Ingbert, Germany; model RS8–50; [35]; Fig. 1) was used. The flexible foil strip is made of 50-µm thin polyimide with 8 substrate integrated, insulated golden connection

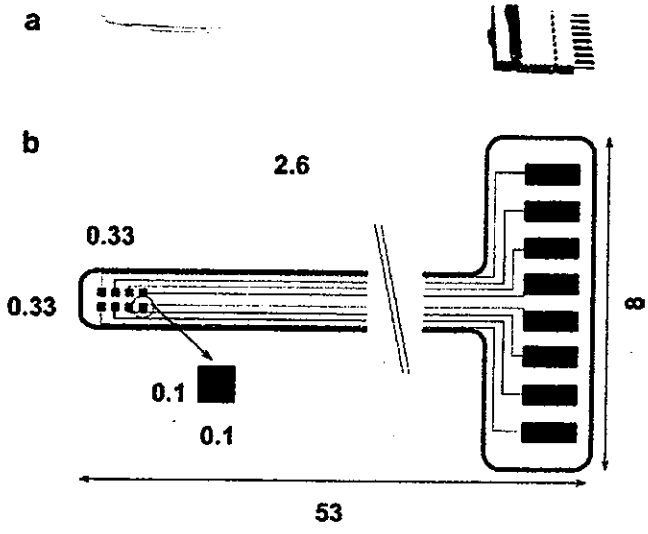

Fig. 1a,b Flexible foil strip for acute subretinal electrical stimulation. **a** The polyimide foil strip (thickness 50 µm, length 53 mm) carries eight platinum electrodes on its tip (*left side*). Each electrode was connected individually through the plug on the right side to an external stimulus generator. The foil strip was used for acute stimulation up to 8 h in final experiments. The tip of the foil was placed in the subretinal space with electrodes facing the overlying retina, the plug outside of the eye. **b** The subretinal foil stimulator with electrode array and contact pads (dimensions in millimeters)

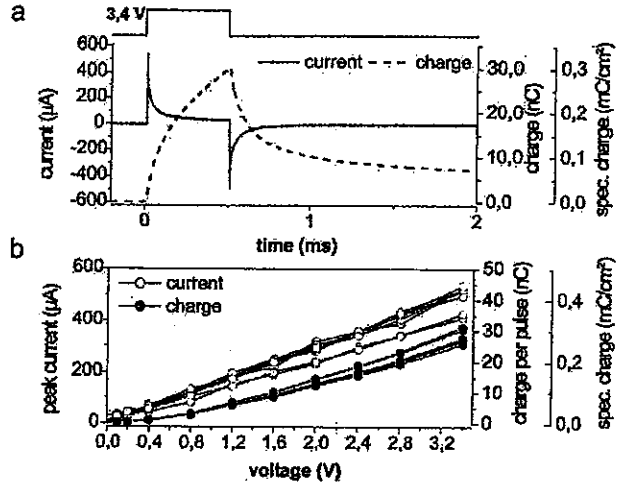

Fig. 2a,b Electrical stimulation with voltage impulses and estimation of injected charge. **a** The current (*bold line*, left scaling) resulting from a voltage pulse (top trace) is measured with a current-to-voltage converter connected between corneal return electrode and ground. By integration of the current trace, the injected charge is estimated and standardized to the electrode area (*broken line*, right scalingsKluwer Academic /Plenum Publishers, New York). **b** Peak current at the raising edge of the voltage pulse and maximum charge reached at the end of the pulse (pulse duration 500 µs) of 8 electrodes of a foil in animal V, plotted against the applied voltage

lanes terminating in a 2×4 array at the end of the strip. Rectangular openings (100×100 μm^2) in the insulation layer at the terminals of the lanes define the size of the stimulation electrodes. The gold electrodes are covered with a thin layer of platinum to enhance the safe charge injection capability. At the other end a plug is soldered to the contact pads to allow connection with the computer-controlled stimulator device (either STG 1008, Multi Channel Systems, Reutlingen, Germany, or function generator HP33120A, Hewlett-Packard, Boeblingen, Germany). Generally biphasic, anodic-first voltage pulses were applied between the subretinally implanted electrodes and a gold-ring contact lens electrode (ERGJet, Universo, La Chaux-de-Fonds, Switzerland) on the cornea serving as large-sized return electrode.

Measurement of charge transfer

The physiologically most common measure of strength of stimulation is "charge injected per pulse", often standardized to the geometric area of the stimulation electrode. To measure the charge transfer through each electrode we estimated in three experiments (animals III, IV, V) the injected charge per voltage pulse and per electrode by measuring the current and subsequent off-line integration of the current transient in each electrode (Fig. 2).

Monophasic voltage pulses (increasing amplitudes up to 3.4 V, pulse duration 500 µs) were applied against ground by a function generator (HP33120A, Hewlett Packard, Böblingen, Germany). The resulting current was measured by means of a current-to-voltage converter that was connected between the corneal return electrode and ground [34].

Preparation for histology

The posterior part of the enucleated eye was immersed in Karnovsky's fixating solution (2% glutaraldehyde, 3% formaldehyde) overnight. Tissue blocs of retina, retinal pigment epithelium (RPE), choroid, and sclera were dissected representing the area of the implantation channel and the area overlying the stimulation electrodes. The specimens were rinsed in phosphate buffer, postfixed in 2% OsO_4 for 2 h at 4°C, dehydrated in graded alcohol, and embedded in epoxy-resin (Epon 812, Science Services, Munich, Germany). Semi-thin sections were stained with Toluidine Blue O (Sigma, Taufkirchen, Germany) for light microscopy.

Results

Implantation of the foils

By using an ab-externo transchoroidal access, a stable subretinal implantation of the electrodes in the area of the visual streaks could be achieved in all ten eyes. Complications from choroidal bleeding did not occur in any case. The retina remained well attached at the area of the electrodes as shown by ophthalmoscopy. In two eyes retinal perforation occurred during and at the site of the incision of the choroid. In these cases, the protruding vitreous was pushed back by an additional epiretinal foil providing good access to the SRS. Thereafter, the subretinal implantation could be performed according to the procedure

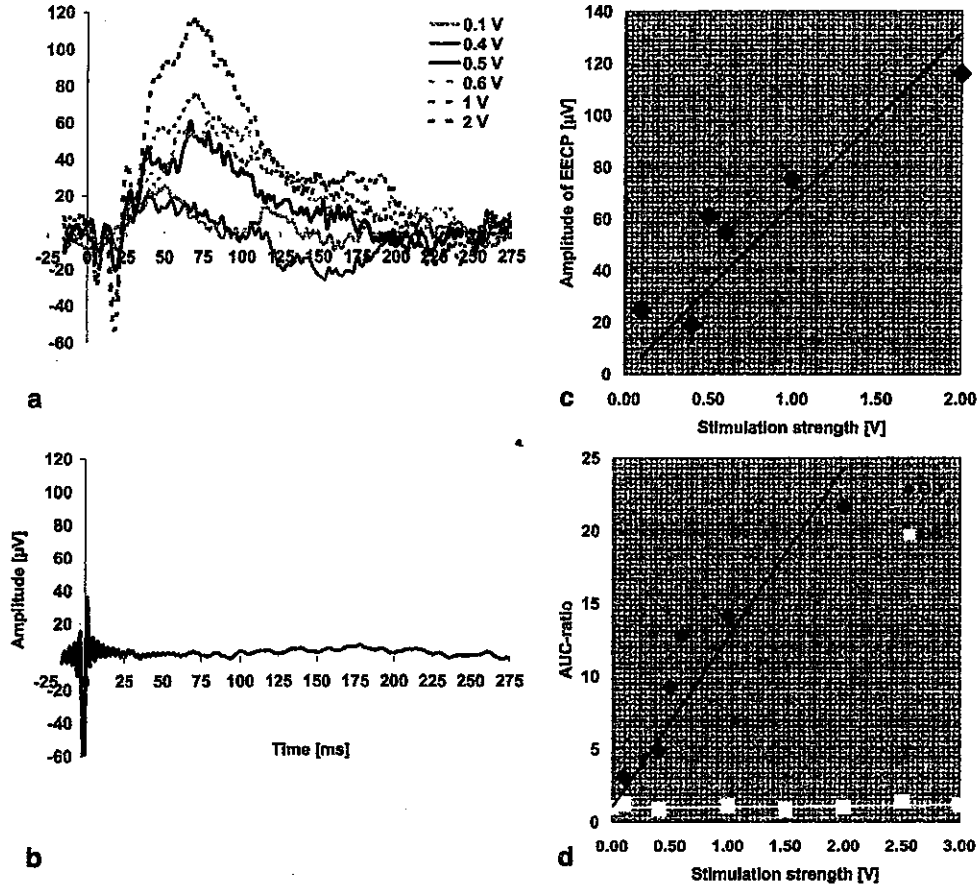

Fig. 3a–d Tracings of electrically evoked cortical potentials (*EECPs*) following subretinal electrical stimulation in rabbit III and evaluation of amplitudes and the area under the curve (*AUC*). **a** In the right eye (first operated eye) a graded response was recorded at 0.1 V (threshold) increasing in amplitude up to 2 V. **b** Even stimulation with 3 V did not lead to discernible cortical responses in the left eye. **c** Relationship of amplitude of EECP and stimulation strength (rabbit III OD; in OS no discernible waveforms were recordable). The amplitude of the cortical response increased with increasing stimulation strength, starting with 25 µV at 0.1 V and reaching 116 µV at 2 V. **d** Relationship of the AUC ratio and stimulation strength in rabbit III (OD and OS). For quantification of cortical responses the AUC ratio was calculated by dividing the AUC of the time where a response was expected (25–200 ms) by the AUC of the noise

described above without hampering the subsequent investigations.

Visual and electrically evoked cortical potentials

The major positive peak of the VEP culminated usually at 90 ms implicit time with some inter-individual variation and did not show significant differences before and after electrical stimulation or surgery.

Cortical recordings following subretinal electrical stimulation of the right and left eye of rabbit III are given illustratively in Fig. 3a,b, respectively. The amplitudes of the major positive peak at the tested stimulation amplitudes are shown in Fig. 3c. At 0.1 V a clearly discernible waveform was detected with an amplitude growing up to 2 V stimulation strength. 0.1 V correspond to a charge transfer value of approximately 1.0 nC per electrode or 10 µC/cm^2 (Fig. 2). The AUC ratios of rabbit III are shown in Fig. 3d. In the right eye a linear regression analysis was performed to calculate the intersection with the null-stimulus line. This intersection has been used to determine thresholds for electrical stimulation before (e.g. [13]). It is necessary to determine the threshold in order to be able to use the entire dynamic range which was at least 1.3 log units (0.1–2 V); however, to find a clearly detectable response we decided to use a higher AUC ratio of greater than 2.0 as a threshold which corresponded well with clearly discernible waveforms throughout our study.

The stimulation strengths at the point where the linear regression exceeded AUC ratio=2.0 for all experiments are given in Table 1. Thresholds ranged from 0.09 to 2.38 V, corresponding to approximately 1 nC per electrode or 10 µc/cm^2 to 17 nC per electrode or 170 µC/cm^2, respectively (Fig. 2; Table 1). Average stimulation threshold for the seven successful eyes was 0.94 V, corresponding to less than 5 nC per electrode or 50 µC/cm^2. Three eyes did not show discernible waveforms at the highest voltage used (3 V) and were thus classified as non-successful. The amplitude of the cortical responses was in average 28±27 µV with an average implicit time of 73±19 ms.

Histology

Histology showed some abrasion of the PRs' outer segments and partial disruption of the monolayered RPE in the area of the implantation channel. After repeated

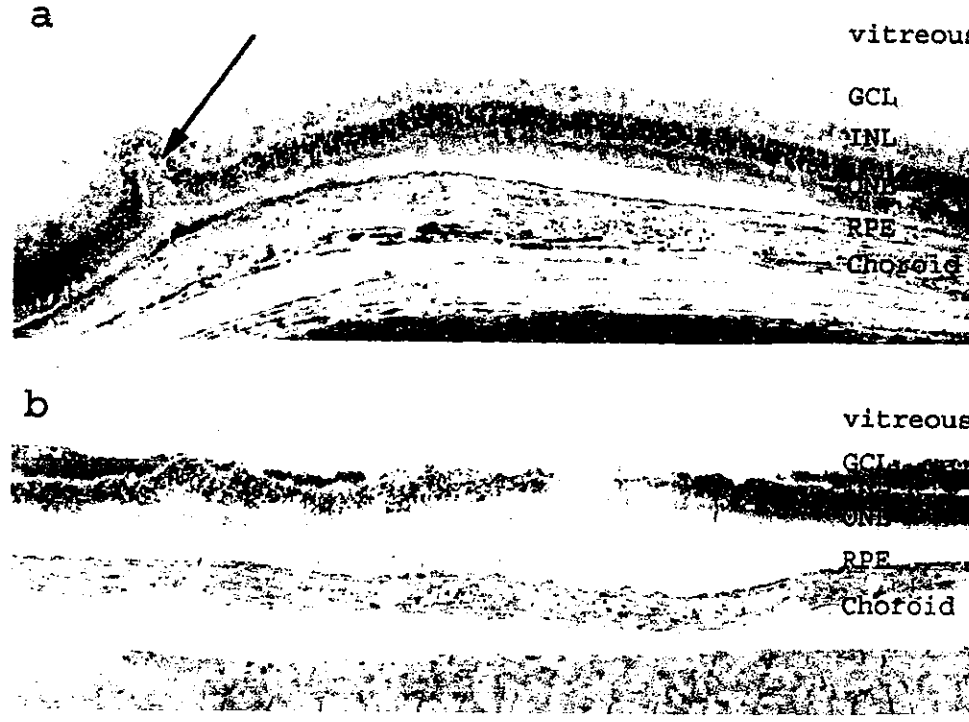

Fig. 4a,b Histological preparation (magnification ×40, Toluidine Blue staining) of a retina after extended stimulation with 2 V (**a**) and 3.4 V (**b**). **a** After repeated stimulation with 2 V, a local retinal lesion developed in the area above an electrode. The photoreceptors and their outer segments are partially destructed and vacuolization of the outer retinal layers is evident (*arrow*), whereas the inner retinal surface and the surrounding retina appear intact. **b** In contrast, 3.4 V-stimulation led to a destruction of all retinal layers. *GCL* ganglion cell layer, *INL* inner nuclear layer, *ONL* outer nuclear layer, *RPE* retinal pigment epithelium

Table 1 Stimulation thresholds based on a linear regression analysis of the area under the curve (AUC) ratios of all ten eyes. Thresholds were calculated using a linear regression analysis of the AUC ratio in each eye. In seven eyes the threshold was calculated to be between 0.09 and 2.38 V. In the other three eyes with no discernible waveforms thresholds read "null"

Rabbit	Eye	Thresholds (V)
I	OD	0.41
I	OS	2.06
II	OD	Null
II	OS	0.63
III	OD	0.09
III	OS	Null
IV	OD	0.56
IV	OS	0.48
V	OD	2.38
V	OS	Null
Average		0.94

stimulation with more than 2 V, the retinal area adjacent to some of the electrodes showed local destruction starting in the outer retinal layers with vacuolization of the PRs' outer segments (Fig. 4a). Stimulation strengths of more than 3 V consistently led to a destruction of all retinal layers (Fig. 4b).

Discussion

In all ten rabbit eyes electrode foils could be implanted into the SRS via the transchoroidal access. Even in eyes with an iatrogenic retinal break at the site of the choroidal incision the electrode could be implanted into the SRS by use of an additional guiding foil to keep back the vitreous. In the setting of the current acute experiments no long-term complications had to be considered; however, close attention will have to be paid to minimize and treat such an adverse event in human eyes. The position of the foils remained stable and the retina well attached during the complete duration of all experiments. Synthetic vitreous substitutes for acute apposition of the retina or for long-term vitreous substitution, which might influence retinal integrity, were not required. No previous detachment of the retina by a liquid bleb was necessary, ensuring the closest possible contact between retina and electrode array in acute experiments. This surgical technique may offer advantages over the classical, transvitreal three port-pars plana surgical technique by possibly avoiding many of the risks and late complications of an intraocular procedure such as endophthalmitis, proliferative vitreoretinopathy, etc. Certainly, more experience has to be gained in other animal models to be able to judge possible use of this method in humans. The surgical technique presented here may be part of the final, complex surgical procedure for long-term implantation of subretinal devices in humans, especially with external epi- or subscleral components which might be necessary for energy supply or larger electronic parts. The unchanged amplitudes and latencies of the VEP before and after surgery and stimulation indicate that the whole procedure did not harm the global retinal and visual pathway function.

Table 2 Excitation thresholds to electrical retinal stimulation in previous

Study	Subject	Sample number[a] (eyes)	acute or chronic	Stimulation					
				site	character				
					device[b]	size of each device	surface area of the stimulus device	delivery system	monopolar or bipolar	phase/form of balance
Doty & Grimm (1962)	cat	appr. 50	acute	transretinal	nicrome electrodes	200 µm diam.		stimulus generator	bipolar	
Dawson & Radtke (1977)	cat	2	chronic (10 months)	epiretinal	three nickel-chrome electrodes	25 µm diam.		stimulus generator	monopolar	monophasic /voltage
Humayun et al. (1994)	bull-frog (in vitro)	12	acute	epiretinal	two platinum electrodes attached to hand piece	75-200 µm diam. (max.1.26x10-7m2)		stimulus generator	bipolar	biphasic /current
	normal rabbit	8	acute							
	rabbit with retinal degeneration[c]	3	acute							
Humayun et al. (1996)	human	8 (RP;6, AMD;1, RD;1)	acute	epiretinal	Three kinds of electrodes[f] attached to hand piece	50 - 200 µm diam.		stimulus generator	monopolar and bipolar	biphasic /current
Chow et al. (1997)	rabbit	3	acute	subretinal	strip electrode[g]		36 mm^2	via photodiode	bipolar	
Humayun et al. (1999)	human	10 (RP;9, AMD;1)	acute	epiretinal	platinum electrode attached to hand piece (1-3)	25-125 µm diam.		stimulus generator	bipolar	biphasic /current
					platinum MEA (3x3, 5x5)	400 µm diam.				
Rizzo et al. (1999)	rabbit	39	acute	epiretinal	gold MEA (5x5)				monopolar / bipolar	
Hesse et al. (2000)	cat	4	chronic (<1 week)	epiretinal	MEA (1x4, 2x4)	0.01 mm^2		stimulus generator	monopolar	biphasic /current
Stett et al. (2000)	chicken (in vitro)		acute	subretinal	MEA[j] (8x8)	10 µm diam.		stimulus generator		monophasi /voltage
Gekeler et al. (this study)	rabbit	10	acute	subretinal	gold with platinum MEA (2x4)	0.01 mm^2	0.08 mm^2	stimulus generator	monopolar	biphasic /voltage

Amplitudes of cortical responses were generally much smaller in response to topical electrical stimulation as compared with ganzfeld light stimulation (VEP). This can be attributed to the total stimulated area: with ganzfeld light stimuli approximately 1000 mm^2 of retina are stimulated simultaneously, whereas the electrodes on the foil strip comprised an area of less approximately 0.5 mm^2.

The dynamic range in our experiments for electrical stimulation of the retina ranged from 0.1 to 1.3 log units (0.09–2 V and 2.38–3 V, respectively; see Table 1). Possible reasons for the intra- and inter-individual difference in dynamic range include the different position of the electrodes on the retina, the different localization of cortical electrodes, differing cortical foldings of the rabbit brain, and differing susceptibility of retinal areas to electrical stimulation as well as saturation effects. We intentionally decided not to exceed 3 V because harm to the retina through physico-chemical effects was expected, thereby possibly reducing the calculated dynamic range. Some saturation effects can already be observed at 2 V (Fig. 3d). A linear regression fit was used nevertheless in order to calculate thresholds. The dynamic ranges of our experiments with electrical stimulation correspond well to reports of VEP V-log I functions [42] showing that subretinal electrical stimulation can make use of a similar dynamic range to produce phosphenes.

After repeated stimulation with more than 2 V the retina adjacent to some of the electrodes suffered from local destruction in the outer retinal layers with vacuolization of the PRs' outer segments (Fig. 4a). Stimulation

Table 2 (continued)

Study	Stimulation parameter: pulse frequency	Stimulation parameter: intensity (voltage or current)	Stimulation parameter: duration	Recording: site	Recording: method	Results: success rate	Results: threshold[c]: intensity (voltage or current)	Results: threshold[c]: total charge (coulombs)	Results: threshold[c]: charge density (C cm^{-2})
Doty & Grimm (1962)	0.3 Hz	1 - 15 V	0.1 - 1.0 ms	optical tract and visual cortex	EECP		less than 1.0×10^{-1} A		
Dawson & Radtke (1977)	0.2 Hz or more	up to 3 mA	0.8 ms, 50 ms	visual cortex	EECP		3.0×10^{-1} A	2.4×10^{-3}	1.63×10^{-3} - 4.89×10^{-3}[d]
Humayun et al. (1994)	1 Hz	50-300 µA	75 ms (half phase)	retinal surface and optic disc	ERG		1.5×10^{-4} A	3.75×10^{-7}	2.98×10^{-4} 8.92×10^{-4} 11.9×10^{-4}
Humayun et al. (1996)	0.5 - 2 Hz	800 µA increasing	0.1 ms increasing	subjective		8 of 8			1.6×10^{-4} - 7.0×10^{-2}
Chow et al. (1997)				visual cortex	cortical response	3 of 3			2.8×10^{-3}
Humayun et al. (1999)			up to 2 ms (half phase)	visual cortex and subjective[h]		10 of 10		4.0×10^{-7} - 2.4×10^{-6}[h]	5.4×10^{-4} - 0.04 1.3×10^{-3}[d]
Rizzo et al. (1999)	0.5 - 16 Hz	75 µA 100 µA	200 µs 100 µs	visual cortex	EECP		7.5×10^{-4} A 1.0×10^{-3} A		
Hesse et al. (2000)		10-500 µA	400 µs (half phase)	visual cortex	EECP	2 of 4	3.5×10^{-5} A	1.4×10^{-8}	
Stett et al. (2000)	0.67 Hz	maximum 3 V	500 µs	ganglion cell body	extracellular recording			4.0×10^{-10}[k] 7.0×10^{-9}[l] 4.0×10^{-9}[m]	5.0×10^{-6}[k] 8.75×10^{-5}[l]
Gekeler et al. (this study)		0.1 - 3.0 V	600-2400 µs (total)	visual cortex	EECP	7 of 10	0.09 V	1.0×10^{-7}	1.0×10^{-3}

a: RP retinitis pigmentosa, AMD age-related macular degeneration, RD retinal degeneration of unknown cause, b: MEA multi electrode array, c: values with shadow background are calculated on the basis of data in corresponding literature, d: if the charge serves the value for 3 electrodes, the charge density will be calculated as 1.63×10^{-3}, and if it serves for one electrode the charge density is 4.89×10^{-3}. It is not indicated by the authors, e: authors have used normal rabbits as well as rabbits with experimentally induced outer retinal degeneration, f: authors used gold-plated or platinum electrodes, g: made by connecting gold leaf to thin nickel-chrome wires, h: cortical recording was unsuccessful, thus the threshold was given as the current that could elicit visual perception on patients subjectively, i: this value is for the stimulation with 5x5 MEA, j: authors used gold electrodes which are covered either with platinum black or a thin titanium nitrite, k: spot stimulation, l: square stimulation, m: box stimulation.

strengths of more than 3 V consistently led to a destruction of all retinal layers (Fig. 4b). Usage of the entire dynamic range has to be questioned again under this impression. Studies on different animal models will have to elucidate the upper threshold for long-term electrical stimulation of retinal tissue as it is intended in retinal prostheses in human clinical use. The choice to use a voltage source was driven by the fact that the final subretinal implant will contain thousands of stimulation electrodes with individually voltage-controlled output and because currently there is no realistic technological concept available for fabrication of microchip with low-power consumption for thousands of current sources with individually controlled current outputs.

The average voltage threshold in the present study was less than 0.94 V, corresponding to less than 5 nC per electrode or 50 µC/cm^2 (Fig. 2; Table 1). This threshold charge density was approximately three magnitudes

higher than the threshold in the study by Chow et al. [5] which provides the only other available measurements for in vivo subretinal electrical stimulation experiments. One possible reason is the extreme difference in size of the stimulation device in the SRS: in the present study the area covered by all 8 electrodes was 0.5 as compared with 36 mm^2 in the study by Chow et al. [5]. A smaller implant as used in our study comes closer to clinically useful devices and previous results [5] therefore do not shed much light on implants in these terms. In consideration of the size of the stimulating devices used in this study we consider the results to be of higher clinical importance, although it may imply higher thresholds as measured by VEPs/EECPs. Additionally, we prefer small densely arranged electrodes to achieve optimal spatial resolution.

The threshold in epiretinal stimulation ranges from 3 to 40 mC/cm^2 (Table 2). The average threshold charge density in our study of 50 $\mu C/cm^2$ falls in the lower part of this range. Two of the cited studies were performed in humans without objective proofs of visual perception, where perceptual thresholds should be lower. It could be expected that the threshold in acute subretinal stimulation are higher than that of acute epiretinal stimulation because of the following reasons: firstly, some injury and subsequent edema of the retina is inevitable in subretinal surgery and is certainly connected with accumulation of some interstitial fluid in the SRS and between the electrodes and the retina. Topical edema of the retina was clearly found transiently with optical coherence tomography in vivo [37]. Small amounts of retinal edema will interfere with signal transduction [41]. Moreover, in vitro experiments have shown that even minute amounts of separation in the micrometer range from electrode to tissue will decrease signal transduction enormously. From this point of view, it seems reasonable to expect that the excitation threshold will be significantly lower in chronic implantation when the retina had enough time to recover from surgical trauma. Secondly, according to the "size principal" [1], which states that larger neurons can be more easily excited by electrical current, the smaller distant neurons of the retina should show a higher threshold than the larger retinal GCs. Contrary to this expectation, our results showed that the other way is the case, i.e., the threshold charge density in our study was in the lower part of the range which epiretinal implant experiments yielded. This fact could point to a higher excitability of the distal retina from the SRS.

The disadvantages of acute experiments, such as transient retinal edema, incomplete retinal attachment over the electrodes, and temporary disturbances of the retinal metabolic state, could be overcome by chronic implantation of devices. Different animal models, however, with holoangiotic retina which could stand the blockage of nutrients from the RPE better would have to be chosen. Cats and Yucatan micropigs have been examined by our group. It has been shown that these retinae tolerate a chronic implant without obvious damage [14, 22, 32]. In contrast to epiretinal implants, where the problem of permanent stability arises, experience in subretinal implantations has shown that the implant remains at the original position for years [14, 22, 32, 33, 43, 44, 45, 46, 47].

Conclusion

In conclusion, this study has proven the principal feasibility of eliciting cortical responses (EECPs) by subretinal electrical stimulation with electrode arrays. The novel transchoroidal approach has been highly successful in all experimental animals of this study in providing a way to the SRS aside of the classical, transvitreal access. Although many studies have been successfully performed by our consortium [13, 14, 26, 32, 33, 34, 44, 45, 46, 47], many questions, such as the shape of the phosphenes elicited by the implants, their interpretation by the cortex, andtheir color will have to be answered by volunteers who can report on their perceptions.

Acknowledgements Support for this study was provided by the German Federal Ministry of Education and Research (BMBF; grant no. 01KP0008). We gratefully acknowledge the help of our project partners in this work (Institute for Microelectronics, Stuttgart; Institute for Physical Electronics, Stuttgart; Natural and Medical Sciences Institute, Reutlingen; Fraunhofer-Institute for Biomedical Techniques, St. Ingbert; all Germany). E. Eckert was extremely helpful in surgery and animal care. The Ewald+Karin Hochbaum-Stiftung generously supported our work.

References

1. Baratta R, Ichie M, Hwang SK, Solomonow M (1989) Orderly stimulation of skeletal muscle motor units with tripolar nerve cuff electrode. IEEE Trans Biomed Eng 36:836–843
2. Brindley GS (1955) The site of electrical excitation of the human eye. J Physiol127:189–200
3. Brindley GS (1973) Sensory effects of electrical stimulation of the visual and para-visual cortex in man. In: Jung R (ed) Handbook of sensory physiology, vol 3. pp 583–594
4. Brindley GS, Lewin WS (1968) The sensations produced by electrical stimulation of the visual cortex. J Physiol Lond 196:479–493
5. Chow AY, Chow VY (1997) Subretinal electrical stimulation of the rabbit retina. Neurosci Lett 225:13–16
6. Crapper DR, Noell WK (1963) Retinal excitation and inhibition from direct electrical stimulation. J Neurophysiol 26:924–947